Dynamic analysis and SDRE control applied in a mutating autocatalyst with chaotic behavior

DYNAMIC ANALYSIS AND SDRE CONTROL APPLIED IN A MUTATING AUTOCATALYST WITH CHAOTIC BEHAVIOR

Dana I. Andrade
Department of Production Engineering, Federal University of Technology-Paraná, Paraná-Doutor Washington Subtil Chueire St. 330, Ponta Grossa 84017-220, Brazil; dana@alunos.utfpr.edu.br

Stefania Specchia
Department of Applied Science and Technology, Politecnico di Torino, Corso Duca degli Abruzzi 24, 10129 Torino, Italy; stefania.specchia@polito.it

Maria E. K. Fuziki
Department of Chemical Engineering, State University of Maringá, Colombo Ave. 5790, Maringá 87020-900, Brazil; mariafuziki@alunos.utfpr.edu.br

Jessica R. P. Oliveira
Department of Production Engineering, Federal University of Technology-Paraná, Paraná-Doutor Washington Subtil Chueire St. 330, Ponta Grossa 84017-220, Brazil; jessica_do_rocio@hotmail.com

Angelo M. Tusset*
Department of Production Engineering, Federal University of Technology-Paraná, Paraná-Doutor Washington Subtil Chueire St. 330, Ponta Grossa 84017-220, Tel.: +55 42-3220-4800, tusset@utfpr.edu.br

Giane G. Lenzi
Department of Production Engineering, Federal University of Technology-Paraná, Paraná-Doutor Washington Subtil Chueire St. 330, Ponta Grossa 84017-220, Brazil; gianeg@utfpr.edu.br

Abstract: In this work, an autocatalytic chemical reactions model with mutation is investigated, and a nonlinear control is proposed to lead the system to a behavior that maintains the system with a desired behavior and with suppress the chaotic behavior. Numerical results considering a broad analysis of the system parameters confirmed the chaotic behavior using phase portraits, bifurcation diagrams and Lyapunov exponents. An analysis of the system behavior in fractional order considering the Atangana–Baleanu–Caputo operator was performed to include the memory effect in the system dynamics. The numerical results obtained demonstrated that the system is extremely sensitive to variations in the order of the derivative, taking the system from chaotic behavior to periodic behavior with small variations in the order of the derivative. The chaotic behavior of the system is proven in fractional order by the 0-1 test and a scale index based on the wavelets test. The proposed control demonstrated to be efficient in maintaining the main product (ethanol) output concentration at the desired level.

Keywords: Autocatalytic Reactions; Chaos; Nonlinear Control; Fractional Order.

1. INTRODUCTION

Currently, fossil fuels are responsible for meeting most of the global energy demand. However, the limited availability of these resources and the adverse effects

their use causes in the environment have become issues of increasing concern. For this reason, sustainability has gained significant importance in the last decades, with a strong emphasis on renewable energy sources. In this context, ethanol emerges as one of the main bio-based products and an alternative to fossil fuels such as gasoline [1-3].

Ethanol is a biofuel obtained from the fermentation of natural sugars. First-generation ethanol is produced from raw materials such as sugar cane, wheat, corn, and potatoes. However, there are concerns about the availability of these raw materials to meet the growing demand for ethanol, as many of them also serve as food for the population [4]. The production of second-generation ethanol emerges as a solution to this challenge. This ethanol is produced from lignocellulosic residues, renewable raw materials, non-food, low-cost, and widely available [5].

Bioreactors play a vital role in every biological process and are essentially the core of bioprocessing. They are the vessels where chemical reactions or microbial activities take place. The bioreactor's design must guarantee optimal conditions for the bioprocess to achieve greater product concentration and maximize yield [6]. Stirred tank bioreactors (STBRs) are commonly used for ethanol production in laboratory and industrial environments. The continuous stirred tank bioreactor (CSTBR) stands out due to its commercial availability. A CSTBR is a well-mixed bioreactor with agitation provided by stirrers [7, 8].

Because of its favorable mixing conditions, some researchers are exploring the application of STBRs in ethanol production. The work by [9] studied the optimization of ethanol production from carob pod extract using immobilized *Saccharomyces cerevisiae* cells in a stirred tank bioreactor. In their work, [10] performed continuous ethanol fermentation from non-sulfuric acid-washed molasses using the flocculating yeast strain KF-7 in a stirred tank bioreactor. In the study by [11], a stirred tank bioreactor was utilized to convert fruit waste directly into ethanol, employing the marine bacterial strain *Citrobacter* sp. E4.

The growth of microorganisms during the fermentation process is affected by several factors, such as the temperature and pressure inside the reactor, the pH of the solution, and the concentration of dissolved oxygen. Effective control of the process is of great importance since the growth rate of the microorganisms directly affects the quality and quantity of the final product [12].

The control of bioreactors presents a challenge due to the nonlinear kinetics of the processes involved. Additionally, controllers for fermentation bioreactors must exhibit

robustness to handle external disturbances that can induce instability. They also need to compensate for model uncertainty arising from the absence of real-time measurements of the active biomass [13].

The literature provides an overview of the available control techniques for bioreactors. The study by [14] proposed using fuzzy-PI and fuzzy-PID controllers with a split-interval strategy to regulate the temperature inside a fermentation vessel modeled as a continuous stirred tank reactor (CSTR). The work by [15] presented the development of an inferential control scheme based on an adaptive linear neural network (ADALINE) soft sensor to control the fermentation process. In [16], a proportional-integral-derivative (PID) controller was proposed for unstable second-order time delay with RHP zero (USOPDT). The controller developed using this method was subsequently applied to a nonlinear stirred tank reactor (CSTR) model. In [17], a nonlinear control method known as SDRE (State-Dependent Riccati Equation) was presented for temperature control in a bioreactor. The proposed controller regulated the flow of cooling fluid through the reactor jacket. The work of [18] contributed to the understanding of reduced-order control, as the authors proposed an LQR (Linear Quadratic Regulator) control project for temperature control in a bioreactor, in which only the equations representing the temperature variation in the re-actor and jacket were considered. In [19] is considered a fractional-order PID (FOPID) control is applied in temperature control of the bioreactor.

In this context, the present work presents a detailed dynamic analysis and a proposal for controlling the product concentration of an isothermal bioreactor modeled as a CSTR (Continuous Stirred Tank Reactor). Dynamics analysis is performed through time histories, phase portraits, and bifurcation diagrams, including the system in fractional order. Lyapunov exponents, the 0-1 test, and the scale index based on the wavelet test are applied to prove the system's chaotic behavior. A control signal is included in the system to suppress the chaotic behavior of the system and maintain ethanol production at desirable levels, considering the nonlinear SDRE control. The 0-1 test determines a parameter K= [0:1] from the system data. The system is considered chaotic for values of K close to 1, whereas a periodic behavior is considered for values of K close to zero [20]. The wave-let-based scale index determines a parameter i_{scale} = [0:1] from the system data. The system is considered periodic for values of i_{scale} close to 0, whereas, for values of i_{scale} close to 1, a non-periodic behavior is considered [21].

The paper is organized as follows: In section 2, the mathematical modeling for the autocatalytic isothermal bioreactor is presented in integer order and fractional order, and in this section, the algorithm for numerical integration of the system in fractional order for the Atangana–Baleanu–Caputo operator is presented. In session 3, the numerical results of the dynamic analysis of the system are presented, both for integer and fractional order. All bioreactor parameters are considered in the dynamic analysis, and the fractional order variation is from 0.9 to 1.1. This session also presents the numerical results of the proposed control, which aims to control the bioreactor to maintain the desired product's con-centration at a previously determined level. Finally, conclusions are summarized in Section 4.

2. MATERIALS AND METHODS

This section presents the mathematical modeling of the autocatalytic isothermal bioreactor, considering the model in integer order and the system in fractional order. The control proposal is also presented in this section, considering the SDRE nonlinear control.

2.1. Mathematical model

Figure 1 presents the physical model of the autocatalytic isothermal bioreactor investigated in this paper.

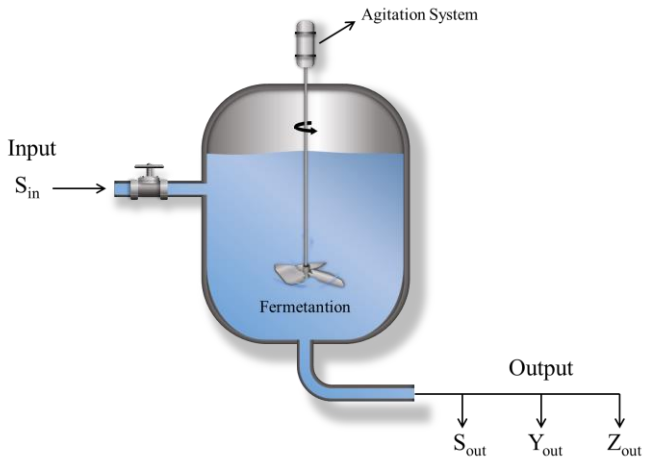

Figure 1- Autocatalytic isothermal bioreactor without feedback control

The conceptual autocatalytic isothermal reaction with mutation that is considered to occur in an isothermal CSTR is described as [22]:

$$
\begin{aligned}
&\mathrm{S+2Y} \xrightarrow{\mathrm{k_1}} \mathrm{3Y} && :(Y \text{ replication})\\
&Y \xrightarrow{\mathrm{k_2}} \mathrm{u_1} && :(Y \text{ decay})\\
&\mathrm{S+2Y} \xrightarrow{\alpha \mathrm{k_1}} \mathrm{2Z+Y} && :(\mathrm{Y\ mutation\ to\ Z})\\
&\mathrm{S+2Z} \xrightarrow{\beta \mathrm{k_1}} \mathrm{3Z} && :(\mathrm{Z\ replication})\\
&Z \xrightarrow[\beta]{\mathrm{k_2}} \mathrm{u_2} && :(\mathrm{Z\ decay})
\end{aligned}
\tag{1}
$$

where: S is the substrate concentration, Y is the desired product concentration (ethanol), Z is the mutant concentration, $\mathrm{u_1}$ and $\mathrm{u_2}$ are the decomposition product concentrations, α is the mutation coefficient, β is the mutation efficiency, θ is the residence time in the reactor, δ is the dimensionless desired product concentration in the feed, k_1 and k_2 are rate constants.

The mass balance equations are obtained from the following equations [22]:

$$
\begin{aligned}
\mathrm{V}\frac{\mathrm{dS}}{\mathrm{dt}} &= \mu\left(\mathrm{S_f}\text{-}\mathrm{S}\right)\text{-}\mathrm{V}k_1\mathrm{SY}^2\text{-}\mathrm{V}\alpha k_1\mathrm{SY}^2\text{-}\mathrm{V}\beta k_1\mathrm{SZ}^2\\
\mathrm{V}\frac{\mathrm{dY}}{\mathrm{dt}} &= \mu\left(Y_\mathrm{f}\text{-}\mathrm{Y}\right)\text{-}\mathrm{V}k_1\mathrm{SY}^2\text{-}\mathrm{V}\alpha k_1\mathrm{SY}^2\text{-}\mathrm{V}k_2 Y\\
\mathrm{V}\frac{\mathrm{dZ}}{\mathrm{dt}} &= \mu\left(Z_\mathrm{f}\text{-}\mathrm{Z}\right)\text{-}\mathrm{V}\beta k_1\mathrm{SZ}^2\text{+}2\mathrm{V}\alpha k_1\mathrm{SY}^2\text{-}\mathrm{V}\frac{k_2}{\beta}Y
\end{aligned}
\tag{2}
$$

where: V is the reactor volume, μ is the specific growth rate, $\mathrm{S_f}$ is the feed substrate concentration, Y_f is the desired product concentration in the feed and Z_f is the mutant concentration in the feed.

System (2) can be rewritten in non-dimensional form after the following substitutions: $x_1 = \frac{\left(\mathrm{S_f}\text{-}\mathrm{S}\right)}{\mathrm{S_f}}$, $x_2 = \frac{Y}{\mathrm{S_f}}$ and $x_3 = \frac{Z}{\mathrm{S_f}}$ [22-23]:

$$
\begin{aligned}
\dot{x}_1 &= -\frac{x_1}{\theta} + \left(1+\alpha\right)\gamma_1\left(1-x_1\right)x_2^2 + \beta\gamma_1\left(1-x_1\right)x_3^2\\
\dot{x}_2 &= \frac{\left(\delta - x_2\right)}{\theta} + \left(1-\alpha\right)\gamma_1\left(1-x_1\right)x_2^2 - \gamma_2 x_2\\
\dot{x}_3 &= -\frac{x_3}{\theta} + \beta\gamma_1\left(1-x_1\right)x_3^2 + 2\alpha\gamma_1\left(1-x_1\right)x_2^2 - \frac{\gamma_2}{\beta}x_3
\end{aligned}
\tag{3}
$$

where: $\gamma_1 = k_1\mathrm{S_f^2}$ and $\gamma_2 = k_2$.

2.2. The mathematical model in fractional order

The dynamic analysis in fractional order considered in this paper is the Atangana–Baleanu–Caputo fractional derivatives with variable order q, and it is assumed that $t_0 = 0$, and $0.9 \le q \le 1.1$. The proposed algorithms [24] are used for constant fractional order parameters. Considering the interval ($0.9 \le q \le 1.1$), the dynamic analysis of the system in fractional order will allow different analyses of the influence of the memory of chemical reactions on the chaotic behavior of the system (3) because, unlike the integer order, the fractional order is a non-local operator that considers in addition to the current state the history of its past state, and can deal with long-range time correlations [25-30].

The fractional autocatalytic isothermal bioreactor system is obtained by replacing the classical derivative with the operator:

$$\begin{aligned}
{}_0D_t^{q_1} x_1 &= -\frac{x_1}{\theta} + (1+\alpha)\gamma_1 (1-x_1) x_2^2 + \beta\gamma_1 (1-x_1) x_3^2 \\
{}_0D_t^{q_2} x_2 &= \frac{(\delta - x_2)}{\theta} + (1-\alpha)\gamma_1 (1-x_1) x_2^2 - \gamma_2 x_2 \\
{}_0D_t^{q_3} x_3 &= -\frac{x_3}{\theta} + \beta\gamma_1 (1-x_1) x_3^2 + 2\alpha\gamma_1 (1-x_1) x_2^2 - \frac{\gamma_2}{\beta} x_3
\end{aligned} \tag{4}$$

Considering the Atangana–Baleanu–Caputo variable-order derivative, we have [24]:

$${}^{abc}_0D_t^q y(t) = f(t, y(t)) \tag{5}$$

Applying the fundamental theorem of fractional calculus in (5) obtain [24]:

$$y(t) - y(0) = \frac{1-q}{\mathrm{b(q)}} f(t, y(t)) + \frac{q}{\Gamma(q)\,\mathrm{b}(q)} \int_0^t f(\rho, y(\rho)(t-\rho)^{q-1} \mathrm{d}\rho \tag{6}$$

where $b(q) = 1 - q + \dfrac{q}{\Gamma(q)}$. Thus, for t_{n+1} we have [24]:

$$\begin{aligned}
y_{n+1}(t) &= y(0) + \frac{\Gamma(q)(1-q)}{\Gamma(q)(1-q)+q} f(t_n, y_n(t)) + \\
&\frac{q}{\Gamma(q) + \mathrm{q}(1-\Gamma(q))} \sum_{m=0}^{n} \int_{t_m}^{t_{m+1}} f(\rho, y(\rho)(t_{n+1} - \rho)^{q-1} \mathrm{d}\rho
\end{aligned} \tag{7}$$

Applying two-step Lagrange polynomial interpolation in the function $f(t_n, y_n(t))$ we have [24]:

$$\mathrm{P_k}(\rho) \simeq \frac{f\left(t_m, y_m\right)}{h}\left(\rho - t_{m-1}\right) - \frac{f\left(t_{m-1}, y_{m-1}\right)}{h}\left(\rho - t_m\right) \tag{8}$$

Substituting (8) into (7), we have [24]:

$$\begin{aligned} y_{n+1}(t) &= y(0) + \frac{\Gamma(q)\left(1-q\right)}{\Gamma(q)\left(1-q\right)+q} f(t_n, y_n(t)) + \\ &\frac{q}{\Gamma(q)+\mathrm{q}\left(1-\Gamma(q)\right)} \sum_{m=0}^{n} \left(\begin{array}{l} \frac{f\left(t_m, y_m\right)}{h} \int_{t_m}^{t_{m+1}} \left(\rho - t_{m-1}\right)(t_{n+1}-\rho)^{q-1} \mathrm{d}\rho - \\ \frac{f\left(t_{m-1}, y_{m-1}\right)}{h} \int_{t_m}^{t_{m+1}} \left(\rho - t_m\right)(t_{n+1}-\rho)^{q-1} \mathrm{d}\rho \end{array} \right) \end{aligned} \tag{9}$$

with [24]:

$$\begin{aligned} a_{q,m,1} &= h^{q+1} \frac{\left(n+1-m\right)^q \left(n-m+2+q\right) - \left(n-m\right)^q \left(n-m+2+2q\right)}{q\left(q+1\right)} \\ a_{q,m,2} &= h^{q+1} \frac{\left(n+1-m\right)^q - \left(n-m\right)^q \left(n-m+1+q\right)}{q\left(q+1\right)} \end{aligned} \tag{10}$$

Integrating (10) and substituting in (9), the following approximation is obtained [24]:

$$\begin{aligned} y_{n+1}(t) &= y(0) + \frac{\Gamma(q)\left(1-q\right)}{\Gamma(q)\left(1-q\right)+q} f(t_n, y_n(t)) + \frac{1}{\left(q+1\right)\left(1-q\right)\Gamma(q)+q} \times \\ &\sum_{m=0}^{n} \left(\begin{array}{l} h^q f\left(t_m, y_m\right)\left(\left(n+1-m\right)^q \left(n-m+2+q\right) - \left(n-m\right)^q \left(n-m+2a\right)\right) - \\ h^q f(t_{m-1}, y_{m-1})\left(\left(n+1-m\right)^q - (\mathrm{n-m})^q \left(n-m+1+q\right)\right) \end{array} \right) \end{aligned} \tag{11}$$

Applying (11) to each equation of system (4), we obtain an algorithm for numerical integration of the system in fractional order:

$$\begin{aligned} x_{1_{n+1}}(t) &= x_1(0) + \frac{\Gamma(q_1)\left(1-q_1\right)}{\Gamma(q_1)\left(1-q_1\right)+q_1} f_1(t_n, x_{1_{n+1}}(t), x_{2_{n+1}}(t), x_{3_{n+1}}(t)) + \frac{1}{\left(q_1+1\right)\left(1-q_1\right)\Gamma(q_1)+q_1} \times \\ &\sum_{m=0}^{n} \left(\begin{array}{l} h^{q_1} f_1\left(t_m, x_{1_m}, x_{2_m}, x_{3_m}\right)\left(\left(n+1-m\right)^{q_1} \left(n-m+2+q_1\right) - \left(n-m\right)^{q_1} \left(n-m+2a\right)\right) - \\ h^{q_1} f_1(t_{m-1}, x_{1_{m-1}}, x_{2_{m-1}}, x_{3_{m-1}})\left(\left(n+1-m\right)^{q_1} - (\mathrm{n-m})^{q_1} \left(n-m+1+q_1\right)\right) \end{array} \right) \end{aligned}$$

(12)

$$x_{2_{n+1}}(t) = x_2(0) + \frac{\Gamma(q_2)\left(1-q_2\right)}{\Gamma(q_2)\left(1-q_2\right)+q_2} f_2(t_n, x_{1_{n+1}}(t), x_{2_{n+1}}(t), x_{3_{n+1}}(t)) + \frac{1}{\left(q_2+1\right)\left(1-q_2\right)\Gamma(q_2)+q_2} \times$$

$$\sum_{m=0}^{n} \begin{pmatrix} h^{q_2} f_2\left(t_m, x_{1_m}, x_{2_m}, x_{3_m}\right)\left(\left(n+1-m\right)^{q_2}\left(n-m+2+q_2\right)-\left(n-m\right)^{q_2}\left(n-m+2a\right)\right)- \\ h^{q_2} f_2(t_{m-1}, x_{1_{m-1}}, x_{2_{m-1}}, x_{3_{m-1}})\left(\left(n+1-m\right)^{q_2}-(\mathrm{n}-\mathrm{m})^{q_2}\left(n-m+1+q_2\right)\right) \end{pmatrix} \tag{13}$$

$$x_{3_{n+1}}(t) = x_3(0) + \frac{\Gamma(q_3)\left(1-q_3\right)}{\Gamma(q_3)\left(1-q_3\right)+q_3} f_3(t_n, x_{1_{n+1}}(t), x_{2_{n+1}}(t), x_{3_{n+1}}(t)) + \frac{1}{\left(q_3+1\right)\left(1-q_3\right)\Gamma(q_3)+q_3} \times$$

$$\sum_{m=0}^{n} \begin{pmatrix} h^{q_3} f_3\left(t_m, x_{1_m}, x_{2_m}, x_{3_m}\right)\left(\left(n+1-m\right)^{q_3}\left(n-m+2+q_3\right)-\left(n-m\right)^{q_3}\left(n-m+2a\right)\right)- \\ h^{q_3} f_3(t_{m-1}, x_{1_{m-1}}, x_{2_{m-1}}, x_{3_{m-1}})\left(\left(n+1-m\right)^{q_3}-(\mathrm{n}-\mathrm{m})^{q_3}\left(n-m+1+q_3\right)\right) \end{pmatrix} \tag{14}$$

where:

$$\begin{aligned} f_1(t, x_1, x_2, x_3) &= -\frac{x_1}{\theta} + \left(1+\alpha\right)\gamma_1\left(1-x_1\right)x_2^2 + \beta\gamma_1\left(1-x_1\right)x_3^2 \\ f_2(t, x_1, x_2, x_3) &= \frac{\left(\delta-x_2\right)}{\theta} + \left(1-\alpha\right)\gamma_1\left(1-x_1\right)x_2^2 - \gamma_2 x_2 \\ f_3(t, x_1, x_2, x_3) &= -\frac{x_3}{\theta} + \beta\gamma_1\left(1-x_1\right)x_3^2 + 2\alpha\gamma_1\left(1-x_1\right)x_2^2 - \frac{\gamma_2}{\beta}x_3 \end{aligned} \tag{15}$$

2.3. Proposal of the control strategy by SDRE control

Considering that systems with chaotic behavior are sensitive to initial conditions, taking the production of ethanol (desired product) to different concentrations without the possibility of predictability, compromising the planning of ethanol production, thus the inclusion of control will make it possible to correct this problem.

Figure 2 shows the bioreactor representation considering the introduction of the control. The proposed control considers the correction of the concentration of variables x_1, x_2 and x_3 through a feedback control that considers the output error.

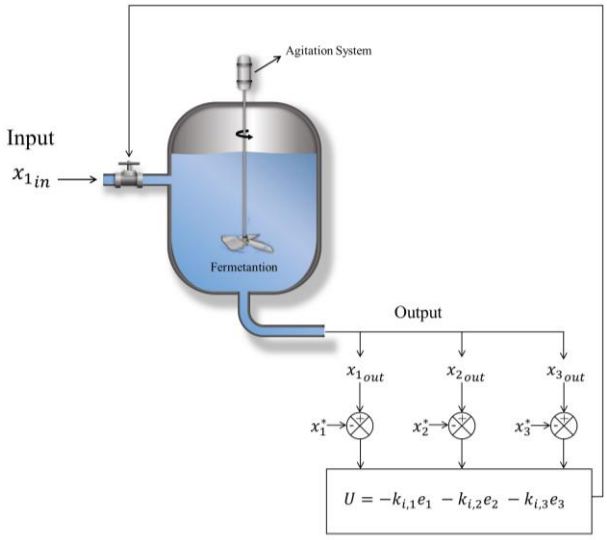

Figure 2 - Autocatalytic isothermal bioreactor with feedback control

The control generally involves parameterizing the variables in an array of states **X**. The SDRE control captures the system nonlinearities with the state coefficient matrix SDC (State-Dependent Coefficient) matrices **A** and **B** [17, 31].

Considering the controlled system in the form of state equations [17, 21, 31]:

$$\dot{\mathbf{X}} = \mathbf{AX} + \mathbf{BU} \tag{16}$$

Where **B** is the control matrix, **A** is the state matrix, and **U** is the feedback control defined as follows [17, 21, 31]:

$$\mathbf{U} = -\mathbf{R}^{-1}\mathbf{B}^{T}\mathbf{Pe} \tag{17}$$

where: $\mathbf{e} = [\mathbf{X} - \mathbf{X}^{*}]$, $\mathbf{X}$ represents the states of the system and $\mathbf{X}^{*}$ the desired states.

The matrix **P** is obtained by solving the Ricatti equation defined as follows [17, 21, 31]:

$$\mathbf{A}^{T}\mathbf{P} + \mathbf{PA} - \mathbf{PBR}^{-1}\mathbf{B}^{T}\mathbf{P} + \mathbf{Q} = \mathbf{0} \tag{18}$$

The functional cost for the feedback control problem is given by [17, 21, 31]:

$$J = \frac{1}{2}\int_{t_0}^{\infty} (\mathbf{e}^{T}\mathbf{Qe} + \mathbf{U}^{T}\mathbf{RU})dt \tag{19}$$

Where **Q** and **R** are positive definite matrices.

3. RESULTS

This section presents the dynamic analysis of an autocatalytic isothermal bioreactor, considering unitary order, fractional order, and nonlinear control.

3.1. System dynamic analysis

The parameters $\alpha = [0.26:0.4]$, $\beta = [0.67:0.75]$, $\delta = [0.04:0.1]$, $\theta = [0.1:0.2]$, $\gamma_1 = [400:500]$ and $\gamma_2 = [11:13]$ were considered.

For numerical simulations, Eq. (1) was considered, integrated by the 4th order Runge-Kutta method, with integration step (h=0.01), fixed initial parameters: $\alpha = 0.272$, $\beta = 0.68$, $\theta = 0.10984$, $\delta = 0.067$, $\gamma_1 = 450$, $\gamma_2 = 11.25$ and initial condition $x_1(0) = x_2(0) = x_3(0) = 0.01$. The equations presented in [21] were considered to calculate the wavelet-based scale index test. For the 0-1 test, the equations presented in [20] were considered. The bifurcation diagram with the maximum displacements and largest Lyapunov exponents were obtained using the algorithms available in [31].

In Figure 3, are present the bifurcation diagrams, considering the parameter $\alpha = [0.26:0.4]$.

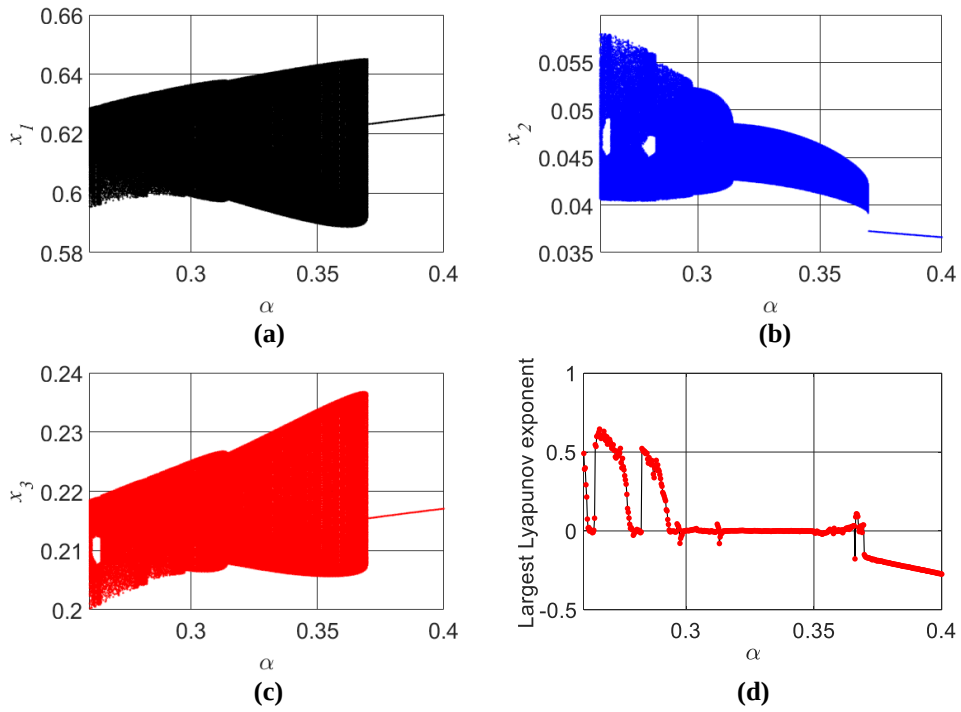

Figure 3 - Bifurcation diagrams and largest Lyapunov exponent for $\alpha = [0.26:0.4]$ case. (a) Bifurcation diagrams for α versus x_1. (b) Bifurcation diagrams for α versus x_2. (c) Bifurcation diagrams for α versus x_3. (d) Largest Lyapunov exponent.

In Figure 4, are present the bifurcation diagrams, considering the parameter $\beta = [0.67 : 0.75]$.

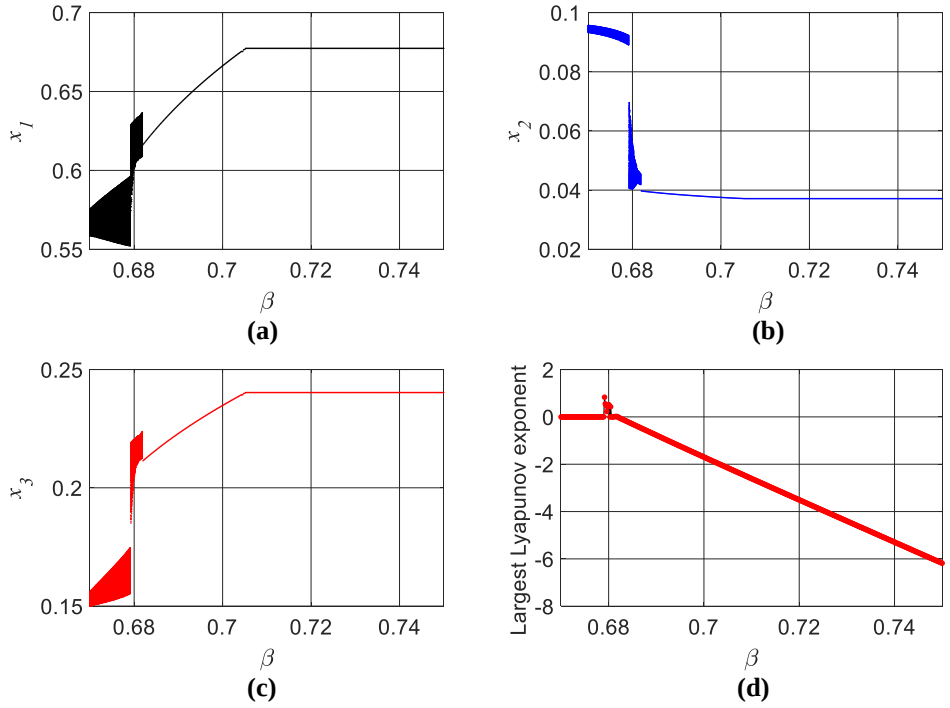

Figure 4. Bifurcation diagrams and largest Lyapunov exponent for $\beta = [0.67 : 0.75]$ case. (a) Bifurcation diagrams for β versus x_1. (b) Bifurcation diagrams for β bversus x_2. (c) Bifurcation diagrams for β versus x_3. (d) Largest Lyapunov exponent.

In Figure 5, are present the bifurcation diagrams, considering the parameter $\delta = [0.04 : 0.1]$.

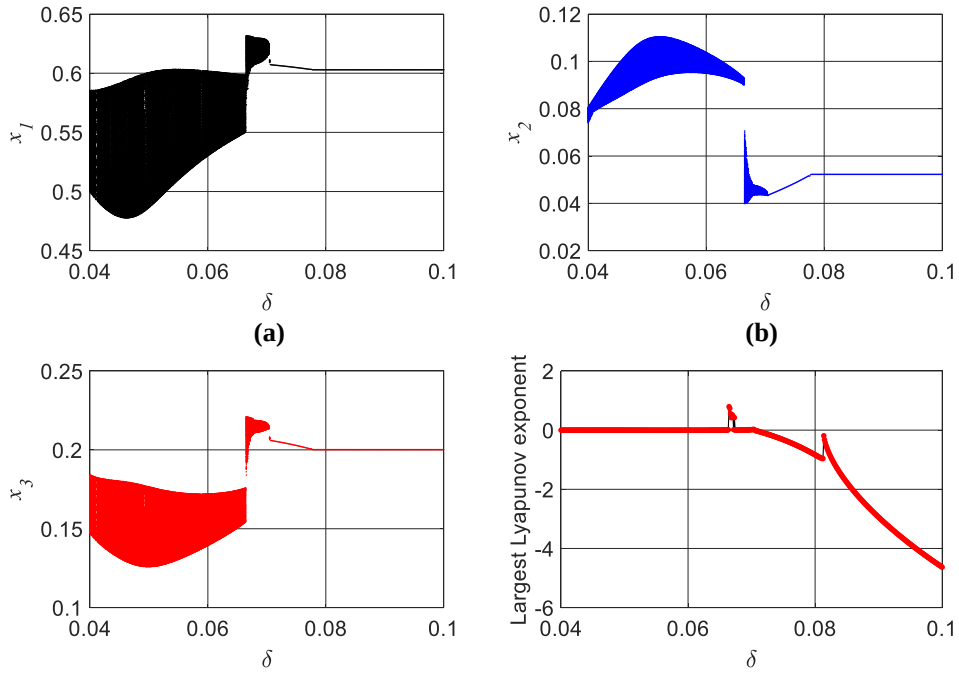

(c) **(d)**

Figure 5. Bifurcation diagrams and largest Lyapunov exponent for $\delta = [0.04 : 0.1]$ case. (a) Bifurcation diagrams for δ versus x_1. (b) Bifurcation diagrams for δ versus x_2. (c) Bifurcation diagrams for δ versus x_3. (d) Largest Lyapunov exponent.

In Figure 6, are present the bifurcation diagrams, considering the parameter $\theta = [0.1 : 0.2]$.

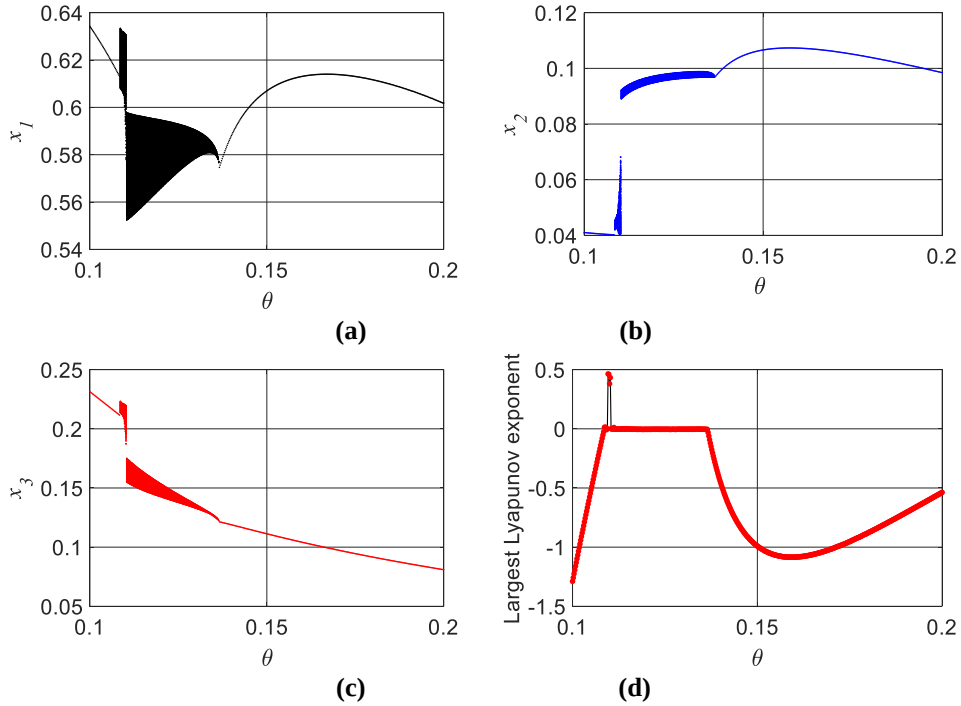

Figure 6. Bifurcation diagrams and largest Lyapunov exponent for $\theta = [0.1 : 0.2]$ case. (a) Bifurcation diagrams for θ versus x_1. (b) Bifurcation diagrams for θ versus x_2. (c) Bifurcation diagrams for θ versus x_3. (d) Largest Lyapunov exponent.

In Figure 7, are present the bifurcation diagrams, considering the parameter $\gamma_1 = [400 : 500]$.

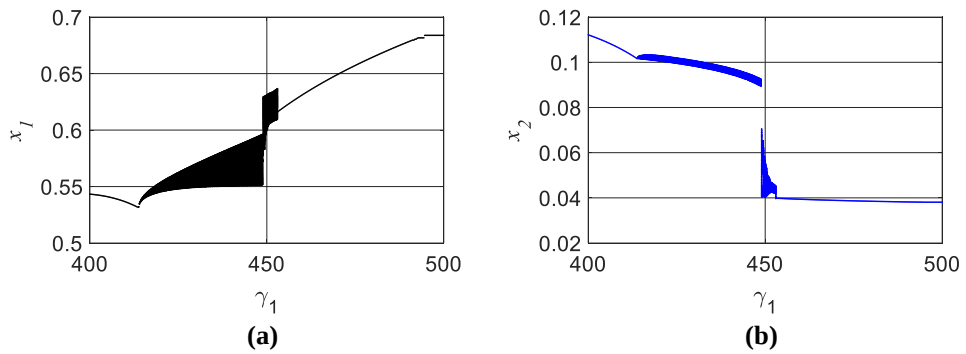

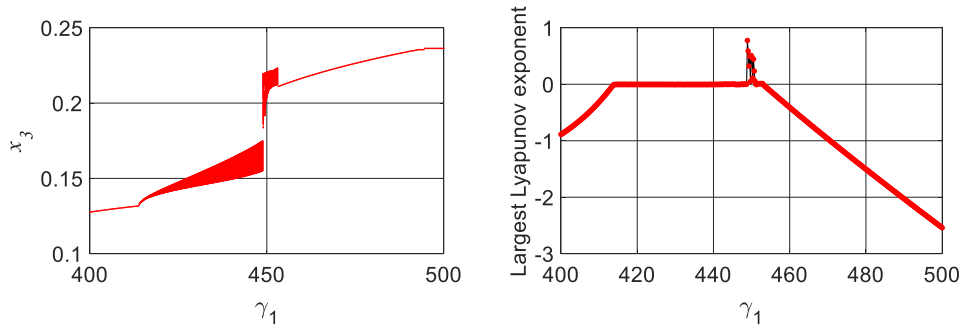

(c) **(d)**

Figure 7. Bifurcation diagrams and largest Lyapunov exponent for $\gamma_1 = [400:500]$ case. (a) Bifurcation diagrams for γ_1 versus x_1. (b) Bifurcation diagrams for γ_1 versus x_2. (c) Bifurcation diagrams for γ_1 versus x_3. (d) Largest Lyapunov exponent.

In Figure 8, are present the bifurcation diagrams, considering the parameter $\gamma_2 = [11:13]$.

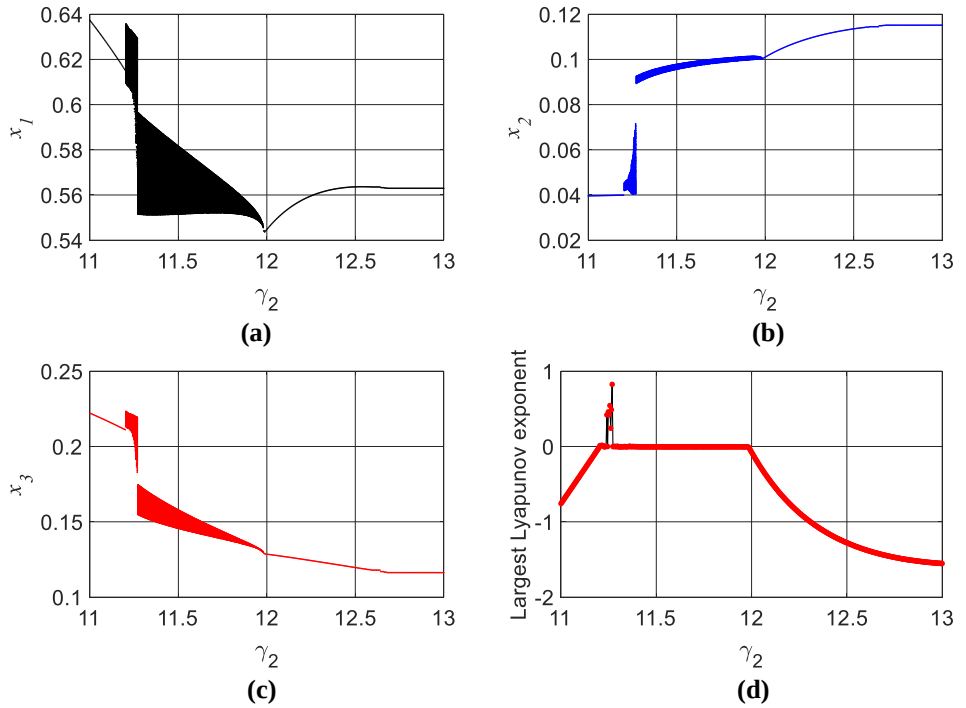

(a) **(b)**

(c) **(d)**

Figure 8. Bifurcation diagrams and largest Lyapunov exponent for $\gamma_2 = [11:13]$ case. (a) Bifurcation diagrams for γ_2 versus x_1. (b) Bifurcation diagrams for γ_2 versus x_2. (c) Bifurcation diagrams for γ_2 versus x_3. (d) Largest Lyapunov exponent.

It is possible to identify a chaotic behavior for the following intervals of the α, β, δ, θ, γ_1, and γ_2 parameters, respectively: α = [0.26:0.2622], α = [0.2639:0.2791], α = [0.2827:0.2934], α = [0.2996:0.3063] and α = [0.3122:0.3127], β = [0.679:0.68]

and β = [0.6811:0.6819], δ = [0.0663:0.0741], θ = [0.1094:0.1104], γ_1 = [448.7:451.1], γ_2 = [11.24:11.27].

Table 1 presents the maximum variations of the desired product (x_2) (in this case, ethanol), considering the parametric variations presented in Figures 3 to 8.

Parameter	Maximum x_2	Largest Lyapunov exponent (λ_1)	Behavior
α = 0.26	0.04-0.057	0.49	Chaotic
β = 0.67	0.0933-0.0956	-0.003	Periodic
δ = 0.052	0.1104-0.0933	-0.002	Periodic
θ = 0.157	0.1073	-1.083	Periodic
γ_1 = 400	0.1120	-0.87	Periodic
γ_2 =12.7	0.1153	-1.446	Periodic

As can be seen in Table 1, if it is possible to use the parameter ($\alpha = 0.272$, $\beta = 0.68$, $\theta = 0.10984$, $\delta = 0.067$, $\gamma_1 = 450$ and $\gamma_2 = 12.7$), the system achieves a better value for (x_2). Therefore, for these parameters, we have a periodic behavior.

In Figure 9a, the historical evolution of the parameters over time is presented: $\alpha = 0.272$, $\beta = 0.68$, $\theta = 0.10984$, $\delta = 0.067$, $\gamma_1 = 450$ and $\gamma_2 = 12.7$. As observed, the behavior is periodic, and as shown in Table 1, the Lyapunov exponent is $\lambda_1 = -1.446$. In Figure 9b, the time history of the parameters is presented $\alpha = 0.272$, $\beta = 0.68$, $\theta = 0.10984$, $\delta = 0.067$, $\gamma_1 = 450$ and $\gamma_2 = 11.25$. As observed, the system exhibits chaotic behavior with a Lyapunov exponent of $\lambda_1 = 0.58$.

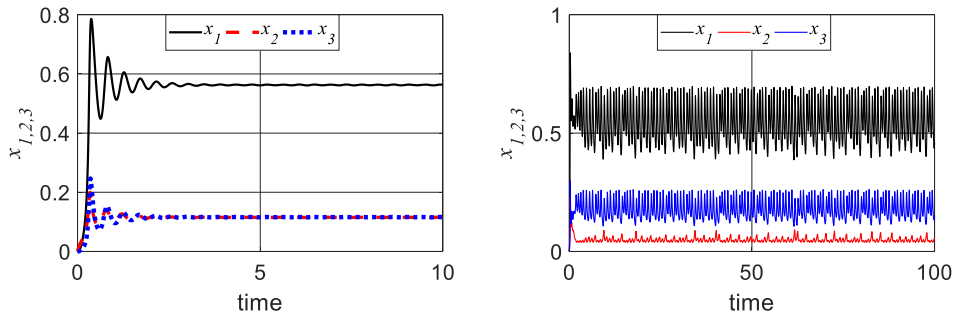

(a) **(b)**

Figure 9. Time history. (a) Time history for the system with periodic behavior. (b) Time history for the system with chaotic behavior.

Figure 10 presents phase diagrams for the system with chaotic behavior, as shown in Figure 9b.

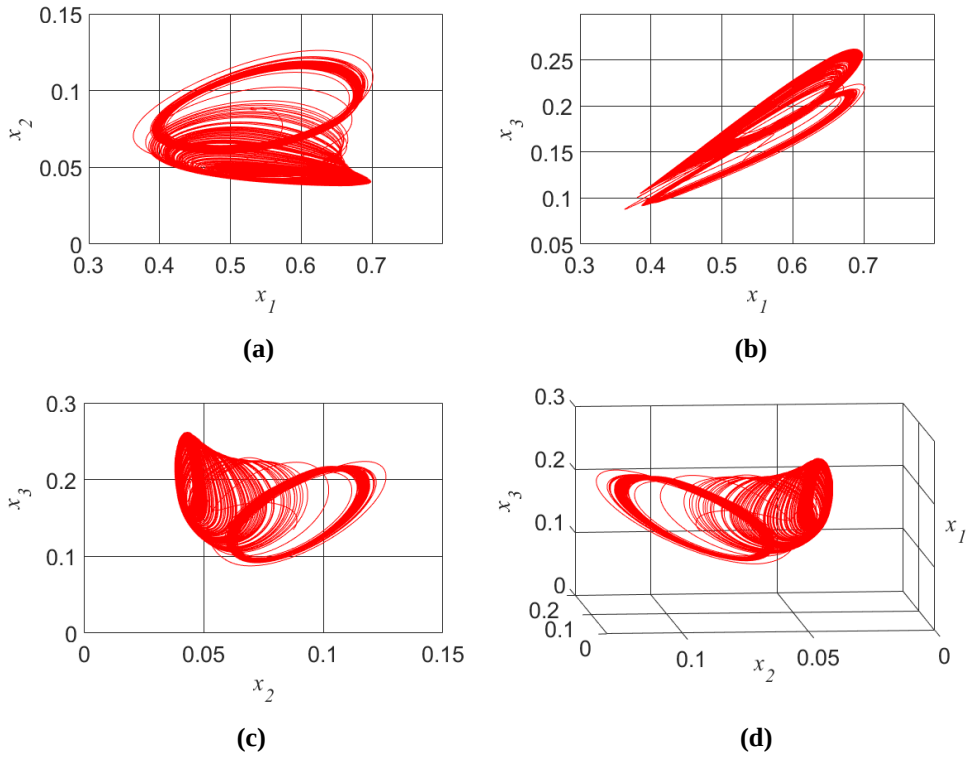

Figure 10. Bifurcation diagrams. (a) Phase diagram x_1 versus x_2. (b) Phase diagram x_1 versus x_3. (c) Phase diagram x_2 versus x_3. (d) Phase diagram x_1 versus x_2 versus x_3.

3.2. Dynamic analysis for fractional order

This section will present the numerical analysis of the influence of the fractional order on the system dynamics, considering slight variations in the entire order of the derivative (q). This analysis seeks to assess the influence of small residues of each component of the bioreactor, evaluating the system's memory. Considering the following variations in the order of the derivative $q_{1,2,3} = [0.09 : 1.01]$. In Figure 11, we present the variation in the fractional order.

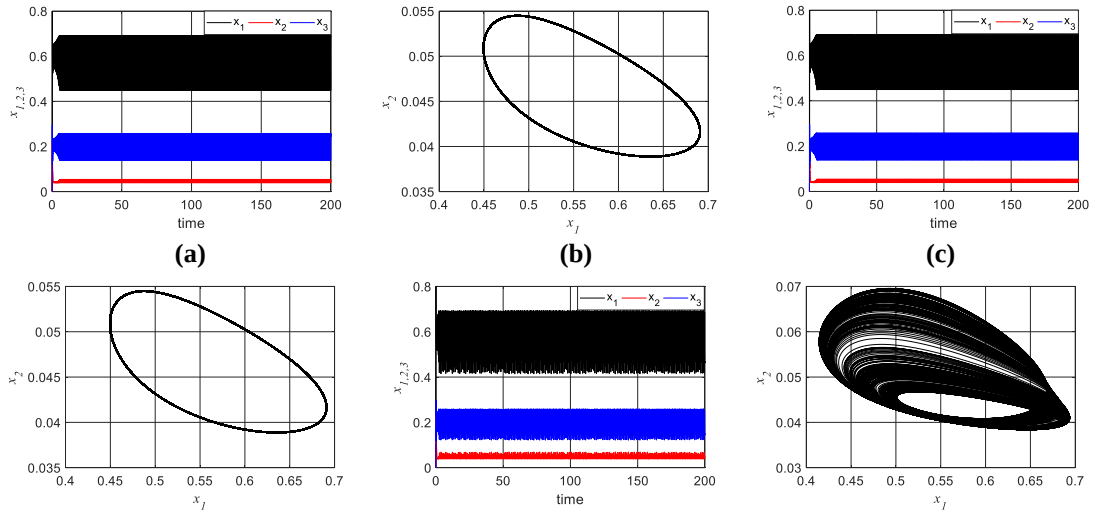

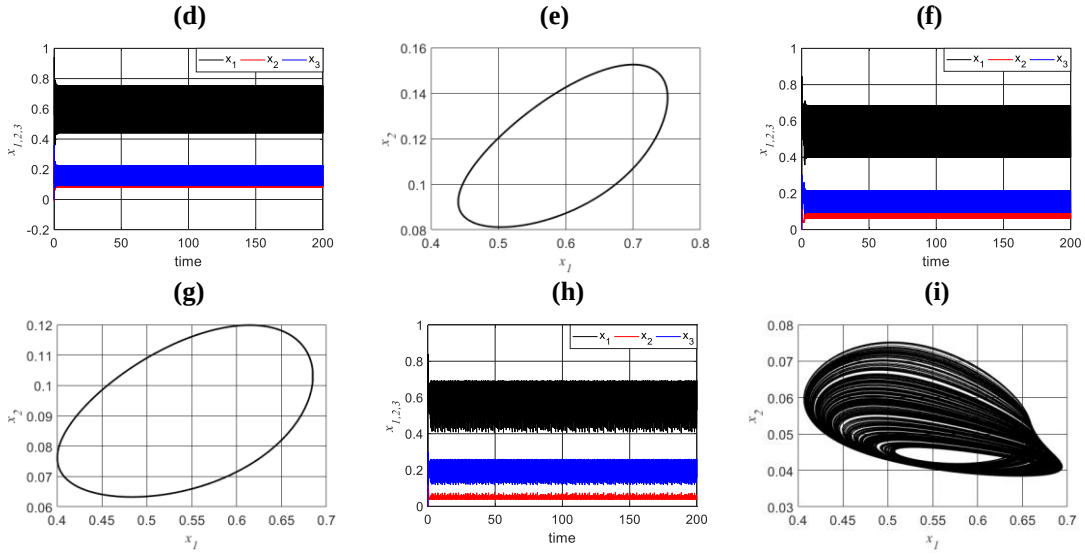

Figure 11. Time history and Phase diagram. (a) Time history and (b) Phase diagram for $q_{1,2,3} = 0.99$. (c) Time history and (d) Phase diagram for $q_{1,2,3} = 0.999$. (e) Time history and (f) Phase diagram for $q_{1,2,3} = 0.9999$. (g) Time history and (h) Phase diagram for $q_{1,2,3} = 1.01$. (i) Time history and (j) Phase diagram for $q_{1,2,3} = 1.001$. (k) Time history and (l) Phase diagram for $q_{1,2,3} = 1.0001$.

As can be seen in the results in Figure 11, the system is sensitive to variations in the order of the derivative. For case $q_{1,2,3} \cong 1$ the system demonstrated that it goes from chaotic to periodic for variations of ± 0.01 or ± 0.001 in $q_{1,2,3}$, returning to chaotic behavior only when it approaches $q_{1,2,3} \cong 1$ again with variations in the order of the derivative. The system is chaotic for $q_{1,2,3} \cong 0.9999$ or $q_{1,2,3} \cong 1.0001$, a behavior proven with the 0-1 test, with a value of $K = 0.96$ and by the scale index based on wavelets with $i_{scale} = 0.87$ for $q_{1,2,3} \cong 0.9999$ and $K = 0.98$ and $i_{scale} = 0.90$ for $q_{1,2,3} \cong 1.0001$.

As seen in Figure 11, the order of the derivative can take the system from a chaotic behavior to a periodic movement or to a fixed point, depending on its variation, behaviors already observed in many systems with chaotic behaviors [21, 31, 25 -30].

3.3. System with SDRE control

As observed in section 3.1, in the case where it is possible to adjust the parameters of the system (1), different behaviors can be obtained, such as periodic or chaotic, as well as driving the system to produce more of the desired product (x_2), in

this case, ethanol. In cases where it is impossible to alter the parameters, including control in one or more variables can be considered.

This section will consider using control to transition the system from chaotic to periodic behavior with increased ethanol production (x_2) achieved through parameter manipulation. The goal is to guide the system from the chaotic behavior presented in Fig. 9b to the periodic behavior with improved ethanol production (x_2), as shown in Table 1 and Fig. 9a.

The system (1) with control can be presented in the following matrix form:

$$\begin{bmatrix}\dot{x}_1\\ \dot{x}_2\\ \dot{x}_3\end{bmatrix}=\begin{bmatrix}-\frac{1}{\theta} & (1+\alpha)\gamma_1(1-x_1)x_2 & \beta\gamma_1(1-x_1)x_3\\ -(1-\alpha)\gamma_1 x_2^2 & -\frac{1}{\theta}-\gamma_2+(1-\alpha)\gamma_1 x_2 & 0\\ -\beta\gamma_1 x_3^2 & 2\alpha\gamma_1(1-x_1)x_2 & -\frac{1}{\theta}-\frac{\gamma_2}{\beta}+\beta\gamma_1 x_3\end{bmatrix}\begin{bmatrix}x_1\\ x_2\\ x_3\end{bmatrix}+\mathbf{BU} \qquad (20)$$

The choice of matrix B determines which system control variables can be performed. Considering the goal of achieving an ethanol production x_2 at a pre-defined level, the inclusion of control in all variables will be considered, starting and maintaining it through variable x_1, as it is the easiest to manipulate in real situations. In this case, we have: $\mathbf{B}=\begin{bmatrix}1\\0\\0\end{bmatrix}$. Defining the desired states $\begin{bmatrix}x_1^*\\x_2^*\\x_3^*\end{bmatrix}=\begin{bmatrix}0.5636\\0.1153\\0.1161\end{bmatrix}$, higher desired product production observed in Table 1, and matrices $\mathbf{Q}=\begin{bmatrix}1 & 0 & 0\\ 0 & 10^4 & 0\\ 0 & 0 & 1\end{bmatrix}$ and $\mathbf{R}=\begin{bmatrix}10^{-4}\end{bmatrix}$.

In Figure 12, the results of the system with the proposed control and without control are presented.

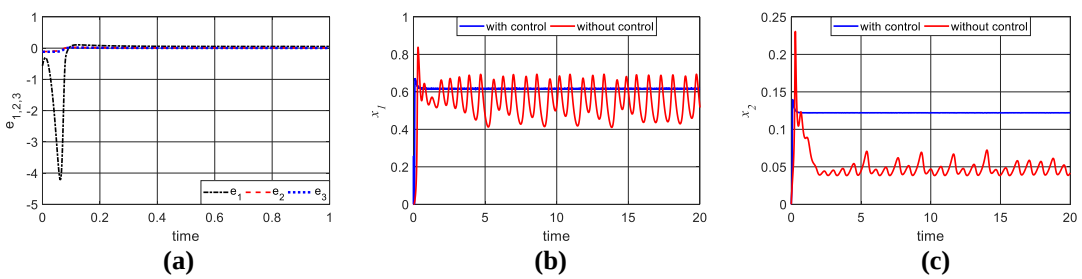

(a) **(b)** **(c)**

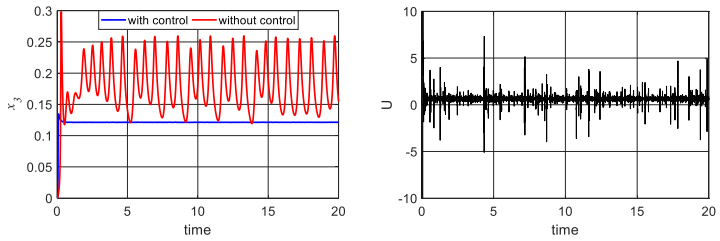

(d) **(e)**

Figure 12. (a) Error $e_1 = x_1 - x_1^*$, $e_2 = x_2 - x_2^*$ and $e_3 = x_3 - x_3^*$. (b) Time history for x_1. (c) Time history for x_2. (d) Time history for x_3. (e) Signal of the control $\mathbf{U}$.

As can be observed in Fig. 12, with the control signal $\mathbf{U}$ (Fig. 12e) applied to the first equation of the system (7), it is possible to control the system, bringing the control error close to zero, as shown in Fig. 12a.

However, considering the case where the goal is to control the ethanol quantity x_2, and in real applications, only variable x_1 (the substrate concentration) can be manipulated, we can conclude that the proposed control efficiently transitions the system from chaotic to periodic behavior with 94.12% accuracy.

4. CONCLUSIONS

The mathematical model of the autocatalytic isothermal bioreactor used in this paper was proposed by [22] and studied by [23]. The authors analyzed the dynamics of the system and the influence of the β parameter on the chaotic behavior of the system. This work contributes to the study of the system proposed by [22], including the study of the dynamics of all system parameters (α, β, δ, θ, γ_1, and γ_2), the investigation of the fractional order considering the influence of memory on the dynamics of the bioreactor. A nonlinear control was also designed to take the system from any initial condition to a desired state.

The numerical results presented in the parametric analysis demonstrated that the system is sensitive to variations in all its parameters, and it was observed in the numerical results that parametric variations can lead to chaotic or periodic behavior. Using the Lyapunov Exponent calculation, it was possible to determine which parameter values the system can lead to chaotic behavior. It was detected that the most influential parameter is the mutation coefficient (α).

Additionally, in the numerical simulations, it was possible to observe that the model investigated represents a self-parametric bioreactor, as even with initial

conditions close to zero, the system presents significant dynamic variations for different parameters. This behavior results from the system's dependence on the parameter δ, representing the dimensionless desired product concentration.

Using fractional order made it possible to analyze the influence of waste accumulated in processes already carried out. These behaviors act as a system memory, influencing future results. The numerical results demonstrated that the system is susceptible to variations in the fractional order, with sensitivity in the order of 10^{-2}.

Considering the sensitivity of the system and the need to maintain ethanol production (x_2) at acceptable levels, it was proposed to include a nonlinear control signal in the system. The numerical results confirmed that the control efficiently keeps the system controlled. The numerical results showed that the lowest error is obtained when the three variables can be controlled. However, for real applications, it is only possible to apply the control to the variable x_1, in this case, the control was efficient in taking the system to a desired behavior with 94.12% accuracy.

Author contributions: Dana I. Andrade, Giane G. Lenzi and Angelo M. Tusset: Conceptualization. **Stefania Specchia:** Methodology. **Angelo M. Tusset:** Software and Formal Analysis. **Jessica R. P. Oliveira and Maria E. K. Fuziki:** Investigation. **Dana I. Andrade, Giane G. Lenzi and Angelo M. Tusset:** Writing-Original Draft. **Stefania Specchia, Jessica R. P. Oliveira and Maria E. K. Fuziki:** Writing-Review & Editing.

Funding: This research received no external funding.

Data Availability Statement: Not applicable.

Acknowledgments: The authors thank the Capes, Fundação Araucária, and CNPq agency. The fifth author thanks CNPq for financial support (process: 310562/2021-0). The last author thanks CNPq for financial support (process: 304068/2022-5).

Conflicts of Interest: The authors declare no conflict of interest.

REFERENCES

1. Rastogi, M.; Shrivastava, S. Recent Advances in Second Generation Bioethanol Production: An Insight to Pretreatment, Saccharification and Fermentation Processes. Renewable and Sustainable Energy Reviews 2017, 80, 330–340. http://dx.doi.org/10.1016/j.rser.2017.05.225

2. Vučurović, D.; Bajić, B.; Vučurović, V.; Jevtić-Mučibabić, R.; Dodić, S. Bioethanol Production from Spent Sugar Beet Pulp—Process Modeling and Cost Analysis. Fermentation 2022, 8, 114. https://doi.org/10.3390/fermentation8030114

3. Damayanti, A.; Bahlawan, Z.A.S.; Kumoro, A.C. Modeling of Bioethanol Production through Glucose Fermentation Using Saccharomyces Cerevisiae Immobilized on Sodium Alginate Beads. Cogent Eng. 2022, 9, 2049438. https://doi.org/10.1080/23311916.2022.2049438

4. Cadiz, J.P.R.; Agcaoili, R.P.; Mamuad, R.Y.; Choi, A.E.S. Fermentation of Sweet Sorghum (Sorghum Bicolor L. Moench) Using Immobilized Yeast (Saccharomyces Cerevisiae) Entrapped in Calcium Alginate Beads. Fermentation 2023, 9, 272. https://doi.org/10.3390/fermentation9030272

5. Vedovatto, F.; Bonatto, C.; Bazoti, S.F.; Venturin, B.; Alves., S.L.; Kunz, A.; Steinmetz, R.L.R.; Treichel, H.; Mazutti, M.A.; Zabot, G.L.; et al. Production of Biofuels from Soybean Straw and Hull Hydrolysates Obtained by Subcritical Water Hydrolysis. Bioresour. Technol. 2021, 328, 124837. https://doi.org/10.1016/j.biortech.2021.124837

6. Novia, N.; Hasanudin, H.; Hermansyah, H.; Fudholi, A.; Pareek, V.K. Recent Advances in CFD Modeling of Bioethanol Production Processes. Renewable and Sustainable Energy Reviews 2023, 183, 113522.

7. Sriputorn, B.; Laopaiboon, P.; Phukoetphim, N.; Uppatcha, N.; Phuphalai, W.; Laopaiboon, L. Very High Gravity Ethanol Fermentation from Sweet Sorghum Stem Juice Using a Stirred Tank Bioreactor Coupled with a Column Bioreactor. J. Biotechnol. 2021, 332, 1–10. https://doi.org/10.1016/j.jbiotec.2021.03.012

8. Karagoz, P.; Bill, R.M.; Ozkan, M. Lignocellulosic Ethanol Production: Evaluation of New Approaches, Cell Immobilization and Reactor Configurations. Renew. Energy. 2019, 143, 741–752. https://doi.org/10.1016/j.renene.2019.05.045

9. Ercan, Y.; Irfan, T.; Mustafa, K. Optimization of Ethanol Production from Carob Pod Extract Using Immobilized Saccharomyces Cerevisiae Cells in a Stirred Tank Bioreactor. Bioresour. Technol. 2013, 135, 365–371. http://dx.doi.org/10.1016/j.biortech.2012.09.006

10. Tang, Y.Q.; An, M.Z.; Zhong, Y.L.; Shigeru, M.; Wu, X.L.; Kida, K. Continuous Ethanol Fermentation from Non-Sulfuric Acid-Washed Molasses Using Traditional Stirred Tank Reactors and the Flocculating Yeast Strain KF-7. J. Biosci. Bioeng. 2010, 109, 41–46. http://dx.doi.org/10.1016/j.jbiosc.2009.07.002

11. Sarkar, D.; Gupta, K.; Poddar, K.; Biswas, R.; Sarkar, A. Direct Conversion of Fruit Waste to Ethanol Using Marine Bacterial Strain Citrobacter Sp. E4. Process Safety and Environmental Protection 2019, 128, 203–210. https://doi.org/10.1016/j.psep.2019.05.051

12. Mohan, V.; Pachauri, N.; Panjwani, B.; Kamath, D. V. A Novel Cascaded Fractional Fuzzy Approach for Control of Fermentation Process. Bioresour. Technol. 2022, 357, 127377. https://doi.org/10.1016/j.biortech.2022.127377

13. Hajaya, M.G.; Shaqarin, T. Multivariable Advanced Nonlinear Controller for Bioethanol Production in a Non-Isothermal Fermentation Bioreactor. Bioresour. Technol. 2022, 348, 126810. https://doi.org/10.1016/j.biortech.2022.126810

14. Fonseca, R.R.; Schmitz, J.E.; Fileti, A.M.F.; Da Silva, F.V. A Fuzzy-Split Range Control System Applied to a Fermentation Process. Bioresour. Technol. 2013, 142, 475–482. http://dx.doi.org/10.1016/j.biortech.2013.05.083

15. Pachauri, N.; Singh, V.; Rani, A. Two Degree of Freedom PID Based Inferential Control of Continuous Bioreactor for Ethanol Production. ISA Trans. 2017, 68, 235–250. http://dx.doi.org/10.1016/j.isatra.2017.03.014

16. Kumar, M.; Prasad, D.; Giri, B.S.; Singh, R.S. Temperature Control of Fermentation Bioreactor for Ethanol Production Using IMC-PID Controller. Biotechnology Reports 2019, 22, e00319. https://doi.org/10.1016/j.btre.2019.e00319

17. Bressan, D.C.; Ribeiro, M.A.; Lenzi, G.G.; Balthazar, J.M.; Tusset, A.M. A Note on SDRE Control Applied in the Fermentation Reactor. Int. Rev. Mech. Eng. 2019, 13, 576–586. https://doi.org/10.15866/ireme.v13i10.17489

18. Tusset, A.M.; Inacio, D.; Fuziki, M.E.K.; Costa, P.M.L.Z.; Lenzi, G.G. Dynamic Analysis and Control for a Bioreactor in Fractional Order. Symmetry 2022, 14, 1609. https://doi.org/10.3390/sym14081609

19. Pachauri, N.; Singh, V.; Rani, A. Two Degrees-of-Freedom Fractional-Order Proportional-Integral-Derivative-Based Temperature Control of Fermentation Process. Journal of Dynamic Systems, Measurement and Control 2018, 140, 071006. https://doi.org/10.1115/1.4038656

20. Tusset, A.M.; Pires, D.B.; Balthazar, J.M.; Fuziki, M.E.K.; Andrade, D.I.; Lenzi, G.G. Dynamic Analysis and Piezoelectric Energy Harvesting from a Nonideal Portal Frame System Including Nonlinear Energy Sink Effect. Actuators 2023, 12, 298. https://doi.org/10.3390/act12070298

21. Tusset, A.M.; Balthazar, J.M.; Rocha, R.T.; Ribeiro, M.A.; Lenz, W.B. On Suppression of Chaotic Motion of a Nonlinear MEMS Oscillator. Nonlinear Dyn 2020, 99, 537–557. https://doi.org/10.1007/s11071-019-05421-8

22. Abasaeed, A.E. Bifurcation and Chaos for a Mutating Autocatalator in a CSTR. Bioprocess Engineering 2000, 22, 337-346. https://doi.org/10.1007/s004490050741

23. Magnitskii, N.A. Universal Bifurcation Chaos Theory and Its New Applications. Mathematics 2023, 11, 2536. https://doi.org/10.3390/math11112536

24. Solís-Pérez, J.E.; Gómez-Aguilar, J.F.; Atangana, A. Novel Numerical Method for Solving Variable-Order Fractional Differential Equations with Power, Exponential and Mittag-Leffler Laws. Chaos, Solitons and Fractals 2018, 114, 175–185. https://doi.org/10.1016/j.chaos.2018.06.032

25. Allahem A.; Karthikeyan, A.; Varadharajan, M.; Rajagopal, K. Computational model of a fractional-order chemical reactor system and its control using adaptive sliding mode control. Fractals 2022, 30, 2240243. https://doi.org/10.1142/S0218348X22402435

26. Yu, Y.; Li, H.X.; Wang, S.; Yu, J. Dynamic analysis of a fractional-order Lorenz chaotic system. Chaos, Solitons and Fractals 2009, 42, 1181-1189. https://doi.org/10.1016/j.chaos.2009.03.016

27. Kheirizad, I.; Tavazoei, M.Saleh; Jalali, A.A. Stability criteria for a class of fractional order systems. Nonlinear Dyn 2010, 61, 153–161. https://doi.org/10.1007/s11071-009-9638-1

28. Li, C.; Peng, G. Chaos in Chen's system with a fractional order. Chaos, Solitons and Fractals 2004, 22, 443–450. https://doi.org/10.1016/j.chaos.2004.02.013

29. Li, C.; Chen, G. Chaos in the fractional order Chen system and its control. Chaos, Solitons and Fractals 2004, 22, 549–554. https://doi.org/10.1016/j.chaos.2004.02.035

30. Petras, I. Fractional-Order Nonlinear Systems: Modeling, Analysis and Simulation; Springer Science & Business Media: Berlin/Heidelberg, Germany, 2011.

31. Tusset, A.M.; Fuziki, M.E.K.; Balthazar, J.M.; Andrade, D.I.; Lenzi, G.G. Dynamic Analysis and Control of a Financial System with Chaotic Behavior Including Fractional Order. Fractal and Fractional 2023, 7, 535. https://doi.org/10.3390/fractalfract7070535

Appendix:

Table 2 - Nomenclature

List of symbols	
A	State matrix
B	Control matrix
P	Ricatti Equation
q	Derivative order
Q	Positive definite matrix
R	Positive definite matrix
J	Functional cost
S	Substrate concentration
Y	Desired product concentration (ethanol)
Z	Mutant concentration
x_1	Substrate concentration in dimensionless form
x_2	Desired product concentration (ethanol) in dimensionless form
x_3	Mutant concentration in dimensionless form
iscale	Scale index
K	0-1 test
Greek letters	
α	Mutation coefficient
β	Mutation efficiency
θ	Residence time in the reactor

δ	Dimensionless desired product concentration in the feed
γ_1	Rate constants
γ_2	Rate constants
Abbreviations	
ADALINE	Adaptive linear neural network
STBRs	Stirred tank bioreactors
CSTBR	Continuous stirred tank bioreactor
CSTR	Continuous stirred tank reactor
PID	Proportional-integral-derivative
USOPDT	Unstable second order time delay with RHP zero
SDRE	State-Dependent Riccati Equation
LQR	Linear Quadratic Regulator
FOPID	Fractional-order-proportional-integral-derivative
SDC	State-Dependent Coefficient